by M. Abrams A. Blusson V. Carrere T. Nguyen Y. Rabu Geologic mapping

The use of satellite data, particularly Landsat images, for geologic mapping provides the geologist with a powerful tool. The digital format of these data permits applications of image processing to extract or enhance information useful for mapping purposes. Examples are presented of lithologic classification using texture measures, automatic lineament detection and structural analysis, and use of registered multisource satellite data. In each case, the additional mapping information provided relative to the particular treatment is evaluated. The goal is to provide the geologist with a range of processing techniques adapted to specific mapping problems.

latroduction

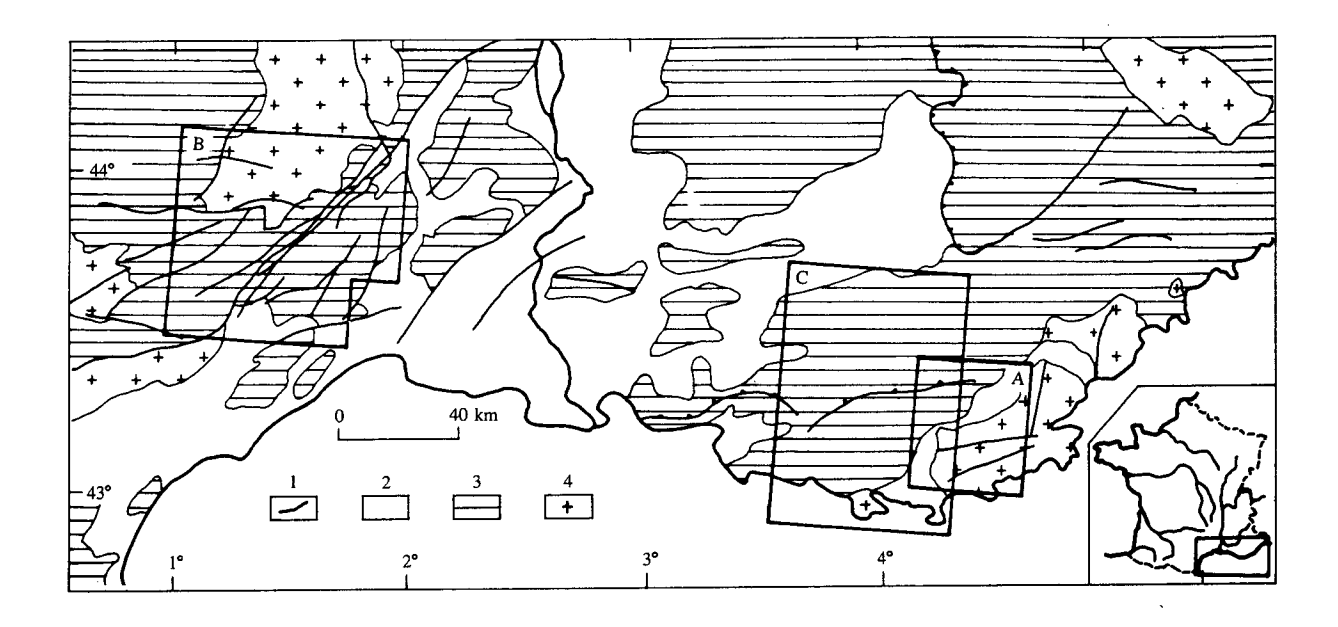
The applications of image processing to remote sensing data for geologic mapping of the earth increased dramatically with the launch of the first Landsat satellite in 1972. The digital format of these data and the prior development of image processing technology for planetary images provided a natural motivation for the early studies of computer-based analyses of earth imagery [1-2]. In addition, geologists were accustomed to using aerial photography and photointerpretation as a tool in geologic mapping. In the beginning satellite images were used in much the same way as standard photographs: An interpreter drew contacts between different units on the basis of tone, geomorphologic characteristics, vegetation cover, etc. The main advantage of

^oCopyright 1985 by International Business Machines Corporation. Copying in printed form for private use is permitted without payment of royalty provided that (1) each reproduction is done without alteration and (2) the Journal reference and IBM copyright notice are included on the first page. The title and abstract, but no other portions, of this paper may be copied or distributed royalty free without further permission by computer-based and other information-service systems. Permission to republish any other portion of this paper must be obtained from the Editor.

satellite images was seen to be their synoptic coverage, presenting large areas of the earth's surface under uniform conditions of illumination and without the boundaries present in standard photo-mosaics. This characteristic was particularly useful for structural analysis, as the continuity of tectonic features was more easily verifiable. This approach, however, failed to take advantage of the digital characteristic of the data, which allows application of enhancement procedures to select and ameliorate the display of that part of the data useful for a particular application. For example, structural analysis of a region is greatly facilitated by images in which faults, fractures, and shear zones appear clearly, without the masking effect of surface cover variations. This can be done with spatial filters, for instance.

The significant advances in image processing technology achieved in the last seven or eight years are attested to by the publication of numerous books dealing with the subject [3-6]. In the specific area of geologic mapping, many techniques detailed in the literature have already proved useful. In general, two geologic themes are treated: lithologic mapping and structural analysis. In this paper we present three new applications of image processing that deal with the problem of creating better images for geologic mapping. In the first part, the use of supervised classification methods for lithologic discrimination is described, with emphasis on the incorporation of spatial information with the radiometric data. In the second part, the application of automatic lineament detection and the generation of rose diagrams are described. The third part discusses the combination of two satellite data sets with widely differing spatial and spectral characteristics. The areas used for the analyses are all found in southeastern France; they are part of a more comprehensive geologic remote sensing study of this region now in progress.

Image processing was performed using the IBM 7350 terminal, a 1024 × 1024-resolution, intelligent color display system with an arithmetic logic unit for performing



Simplified geologic map of southern France with three regions studied (A, eastern Provence; B, Cevennes; C, western Provence). 1, Fault. 2, Alluvium and basins. 3, Sedimentary cover rocks. 4, Basement rocks.

operations on locally stored data [7]. The High-Level Image Processing System (HLIPS) software package performed most of the processing in the local environment. The processing and display device was attached to an IBM Model 3031 computer, providing access to large data files and the capability of performing complex operations in the host if necessary.

Lithologic classification using texture measures

• Introduction, data utilized, and description of area The process of making geologic maps using Landsat data presents the geologist with several problems: characterization of units, their differentiation, and tracing boundaries between them. There are many approaches for processing the image data to provide an improved rendition of the area of interest; in general these fall into two broad categories, image enhancement and classification. The former has as its goal the enhancement of image displays for later photointerpretation; the latter method, with which this study is concerned, seeks to use the computer's ability to process statistical information to automatically assign pixels to a class and produce classification or thematic maps. In addition to using the spectral information, we calculated a texture parameter to incorporate spatial information into the analyses. A supervised classification algorithm, the Bayesian maximum likelihood classifier, was used to produce thematic maps based on training areas. The different maps were combined to produce the final map.

The data utilized were taken from Landsat scene 23834-30046, acquired June 16, 1980. A 40 by 40-kilometer subarea was extracted from the scene for detailed analyses using the four Multi-Spectral Scanner (MSS) bands.

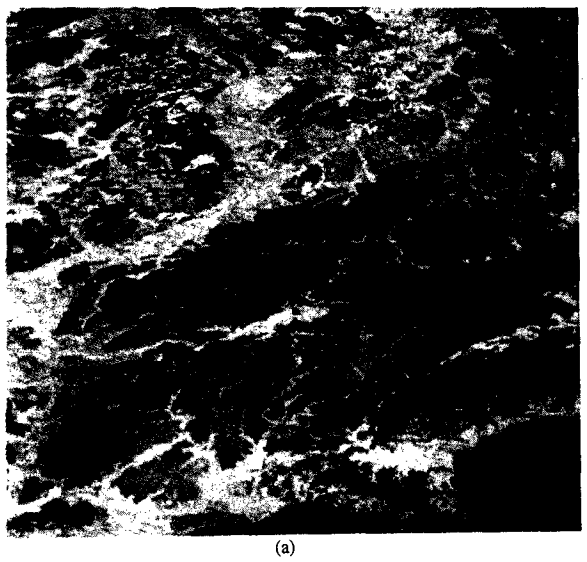
The area studied is located in the eastern part of Provence (A in Figure 1). Basement rocks are represented by a crystalline complex consisting of granites, gneisses, schists, and amphibolites. The younger sedimentary cover consists of volcanic rocks (rhyolites and volcanoclastics), limestones, dolomites, argillites, and alluvium. The structural history is complex: the area was strongly deformed during the Pyrennean orogeny and later during the Alpine orogeny. The basement rocks are characterized by reverse faults, and the cover rocks by thrust faulting and décollements. Physiographically, the area is heavily vegetated, with dense pine forests covering elevated regions. The valleys and basins are moderately cultivated, further masking the underlying lithologies.

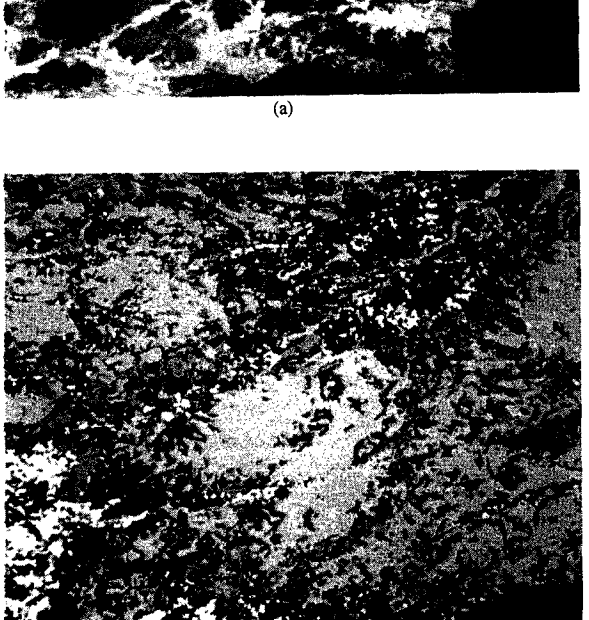
• Processing techniques used

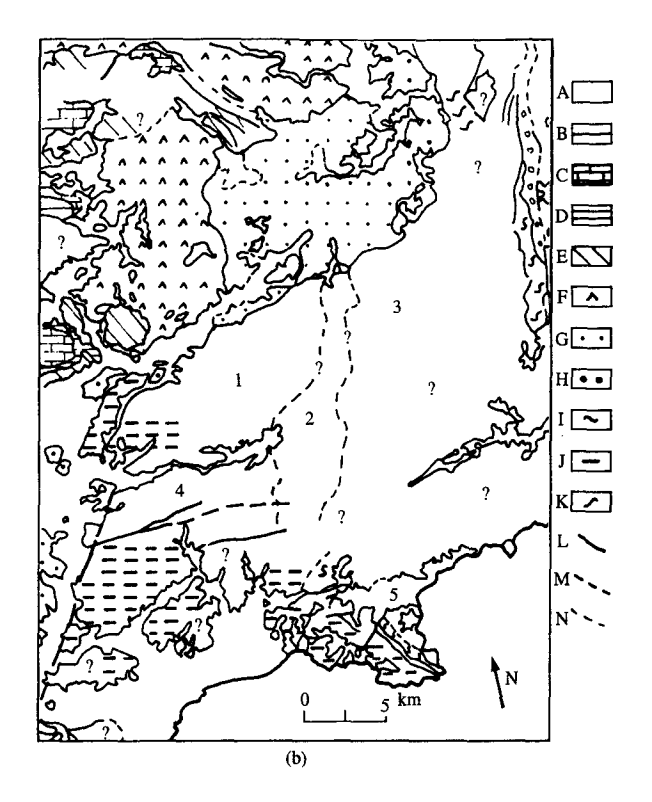
A false-color infrared composite was produced [Figure 2(a)] using MSS bands 4, 5, and 7, and a lithologic interpretation map [Figure 2(b)] was created from this image to serve as a reference for judging the improvements brought by the classification analyses.

Further data processing was performed in the following manner:

• Extraction of spectral characteristics of representative







TOUC2

Eastern Provence region: (a) Landsat false-color infrared composite. (b) Geologic interpretations of (a) and (c): 1, Phyllades; 2, Micaschist; 3, Gneiss; 4, Quartzite; 5, Micaschist. A, Alluvium; B, Jurassic; C, Bathonien; D, Bajocien; E, Lias; F, Triassic; G, Permian; H, Carboniferous; I, Gneiss; J, Phyllades; K, Micaschist; L, Fault; M, Possible fault; N, Possible contact. (c) Composite classification map utilizing masks of intermediate classification maps on which each unit is best classified.

training areas from MSS bands which had been destriped by means of a histogram adjustment technique;

- Creation of segmented images, and extraction of the spectral characteristics of those images by using the same training areas;
- Creation of a texture image, and extraction of texture measures using the training areas;
- Applications of a supervised classification algorithm using the above parameters to produce thematic maps;
- Combination of the classification maps using criteria of concordance, and assessment of accuracies to produce the final map.

Training areas were defined on the image by using the detailed geologic maps as references. The histograms of each class were extracted from the four MSS bands. For those which were bimodal or plurimodal, the training areas were redefined to generate unimodal histograms.

Summary of best classification results.

Unit	MSS	SEG	SEGT
Quartzite	X		
Phyllades			X
Micaschist		X	
Gneiss			X
Permian	X		
Triassic			X
Jurassic			X
Alluvium	X		
Vegetation	X	X	X

MSS-Multispectral scanner data only

SEG-Multispectral scanner data with segmentation.

SEGT-Multispectral scanner data with segmentation and textural information.

From visual interpretation of the color composite, it appeared that lithologic units were heterogeneous on a scale of a few pixels; this was verified in studying the histograms for the training areas. The heterogeneity is due to shadowing, changes in vegetation cover, land use disturbances, etc. In order to homogenize or smooth the images before classification, a segmentation procedure was applied to the data. Previous work [8] demonstrated that this technique effectively improved classification accuracy.

The creation of the segmented image was accomplished by means of a contour extraction program [8]:

 Filtering the image by using a gradient operator to produce an angle image and a gradient image, using the following two kernels successively:

- 2. Elimination of the points where the gradient was not a local maximum in its direction.
- 3. Searching for the nearest neighbors of each point, taking into account the gradient direction. For each point of the contour a predecessor was defined and a successor numbered from 0 to 9 according to their position, 0 corresponding to the absence of a neighbor. A neighbors image was thus created where, for each pixel, the predecessor and the successor were indicated.
- 4. Construction of the contours from the neighbors image, linking the points in such a fashion as to favor those which were more linear. This was done in two steps: 1) Linking a point to its successor if the latter had the former as its predecessor; we thus created a first table of contours containing for each contour the coordinates of its origin and its end, and its length; the neighbors image allowed us to follow the contours. 2) Next, for each contour we determined its predecessor and successor; we linked the contours, following the same rule as for the points. We obtained a new table of contours and

modified the neighbors image by following the contours, taking the shortest route.

Contours more than nine pixels long were retained. These contours were then treated to form closed segments. Finally, the segments were filled with the average radiometric value of the pixels contained within. The segmentation process reduced the intraclass means and increased the interclass means, which should have improved classification accuracy.

A photointerpreter uses spatial information to discriminate units, in addition to the spectral information (tone or color). The spatial information is expressed as texture at a variety of scales and is in general related to the drainage pattern developed on different rock types. We calculated a texture measure by applying a gradient operator to MSS band 6 to detect brightness edges, then filtering this image with a 7 by 7 average filter. The size of the filter was based on examination of the image and on observation that the minimal natural frequency of morphological features observable was on the order of 250 m. This texture image was used as an additional variable for the classifications.

The supervised classifications were done using a Bayesian maximum likelihood classifier. This algorithm is commonly used for classifying Landsat data and has been found to be very effective [9]. The method is based on selection of training areas from which statistics are extracted for the variables (channels). The rest of the image is classified point by point by assigning a pixel to the class which it resembles most closely from a statistical standpoint.

The final classification map was produced in two steps. First, a map was produced from three classification runs by keeping only those pixels which were assigned to the same class on all three; the rest of the area was left unclassified. Second, the blank areas were replaced by class maps chosen from the three classifications after comparison with the geologic maps to determine which classification produced the most accurate result for a particular class. These masks were used to fill in the blank areas on the concordance map.

• Results of classifications

The first classification was done using the original MSS channels, with nine classes defined from training areas. Some of the classes were accurately represented on the thematic map; the majority, however, were misclassified. In addition, the map appeared to have many isolated misclassified pixels, giving an impression of noise. By using the segmented image, all of these isolated pixels were eliminated, and in addition there was an improvement in the accuracy of classification of several classes. The third classification, adding the texture image to the segmented channels, improved the classification, particularly for those classes having similar spectral values but different morphological characteristics.

The final classification map [Figure 2(c)] was produced as described above. The masks were produced from the classifications which were the most accurate on a class-by-class basis (Table 1).

An interpretive geologic map was prepared from the final classification map. After comparison with the interpretation of the false-color composite, the improvements were added to the cartography. They appear in Fig. 2(b) as areas with numerals 1 to 5. Significant areas of the basement massifs are now mappable, where little detail appeared on the color composite. This is due to the effects of the segmentation, which increased the classification accuracy, and to the addition of a texture channel to the spectral data. This methodology combines different image parameters and allows the interaction of the geologist in the selection of the masks to be combined.

Automatic lineament detection and structural analysis

• Introduction, data utilized, and region studied This section describes a comparison between manual and automatic analysis methods for structural studies of Landsat data. Structural analysis of images usually involves the creation of photo-interpretation maps, showing faults, folds, and fractures (where recognizable), and lineaments, or linear and curvilinear features where doubt exists as to the origin of the feature. A standard method of summarizing this information is in the form of rose diagrams, which are polar plots of direction versus frequency of occurrence of faults, fractures, etc. These plots are normally constructed manually; however, we developed a method for automatically extracting linear features from images, then producing rose diagrams for any region desired, including the entire image. The area analyzed is the Cevennes region in southern France (B in Fig. 1).

The primary data used for regional analysis were taken from Landsat scene 22451-29136, acquired October 8, 1981; a 60 by 80-km subarea was extracted for analysis [Figure 3(a)]. MSS band 7 was used for processing because of the minimal atmospheric scattering effects in this wavelength region.

The Cevennes region is located along the southeastern border of the Massif Central, which is underlain by basement rocks consisting of gneiss, schist, and granite. Unconformably overlying part of the basement is a moderately thick sequence of Mesozoic sedimentary rocks, primarily limestones. The dominant structure in the region is the NE-SW-trending Cevennes fault zone. This fault, which has been active since at least the Permian period of the Paleozoic Era, currently demonstrates left lateral displacement. It is thought by some [10] that this feature represents a major transform fault which has greatly affected the tectonic development of southern France since before the

Alpine orogeny. The fault zone is expressed in the topography by a series of subparallel, elongate ridges and valleys that form a zone of disruption tens of kilometers wide. It separates a region of little-deformed cover rocks to the northwest from an area of moderately to intensely deformed sediments to the southeast. Other faults in the area trend east-west and north-south, but are of less tectonic importance.

• Processing techniques used

The algorithm implemented [11] was used to detect structural features having a maximum local brightness gradient. Once these contours were found, several shape parameters were calculated to select appropriate features.

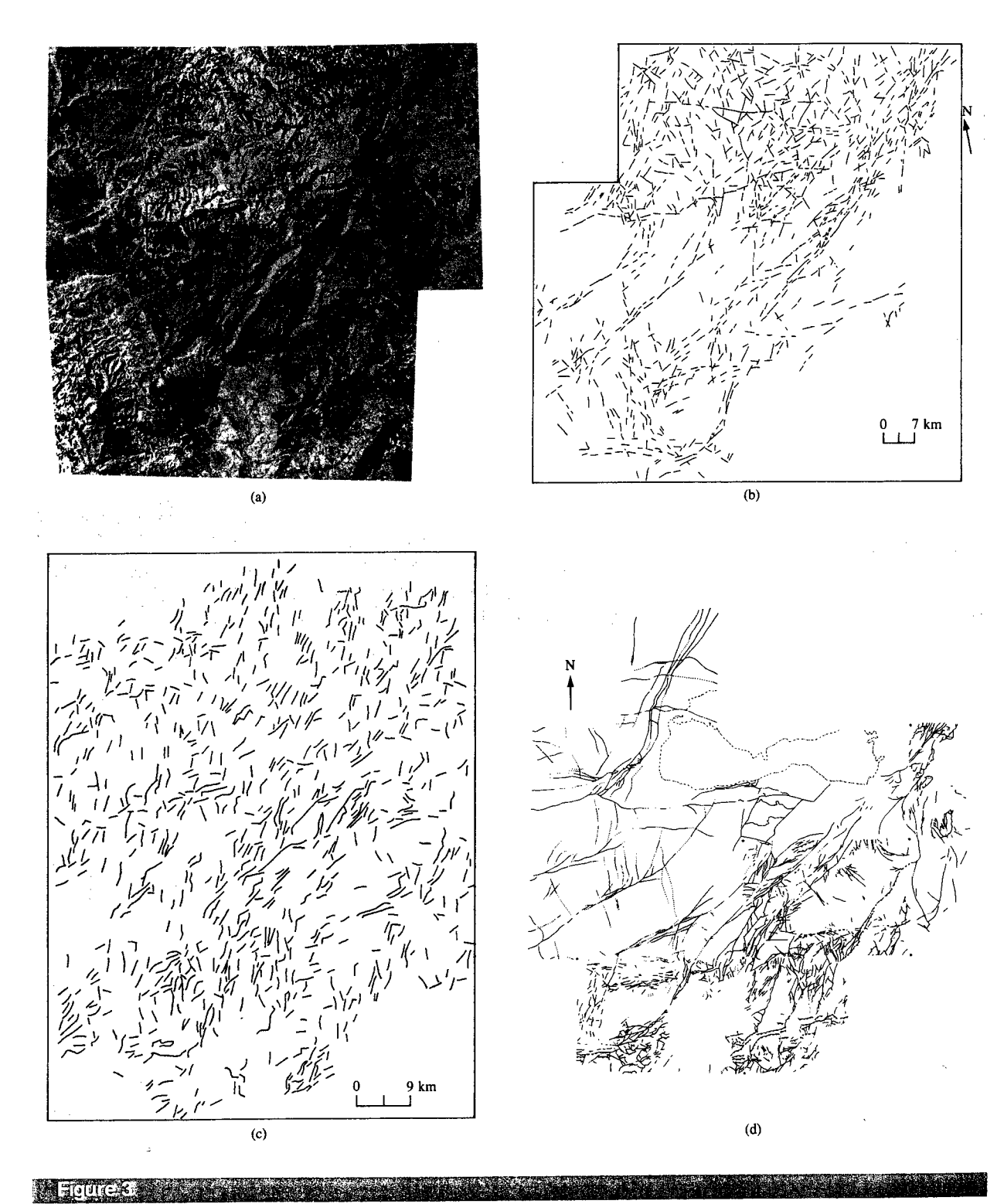
The extraction of contours having a strong local gradient was accomplished by the method described earlier in the section on lithologic classification. This contour image contains all the brightness gradients in the image which are somewhat linear; however, many remain which are curved, meandering, or tortuous in shape. Those of interest in a structural study are the ones which are more or less linear, as most faults and fractures tend to be linear. The undesired contours are eliminated by calculating a criterion of linearity which compares the total length of the contour to the euclidean distance between the end points. This parameter has a value of 1 for a straight line, increasing with the sinuosity and curvature of the line. By selecting an appropriate threshold value, sinuous contours are largely eliminated.

The lineament image thus created was used as a mask for the angle image produced by the gradient program. The new masked angle image was then used to produce the rose diagrams by calculating the frequency of points as a function of angle, regrouping the data into ten-degree classes, and plotting these data in a polar graph. This automatic procedure was applied to the Landsat data, and the rose diagrams were compared with those manually calculated from the same image.

The lineament map produced by standard photointerpretation of the MSS band 7 image was also compared with the lineament image automatically produced using the treatment described above.

Analysis of data

The comparison between the lineament map [Figure 3(b)] and the thresholded contour image [Figure 3(c)] shows that 95% of the lineaments on the MSS 7 interpretation are represented on the contour image, even if only partially. The contour image contains many additional lines which come from relief features, the hydrographic network, etc. All main fault directions are present, as are lineament intersections. The interpreted faults are generally longer than the corresponding contours, the interpretation (morphology) allowing the geologist to link consecutive segments even if



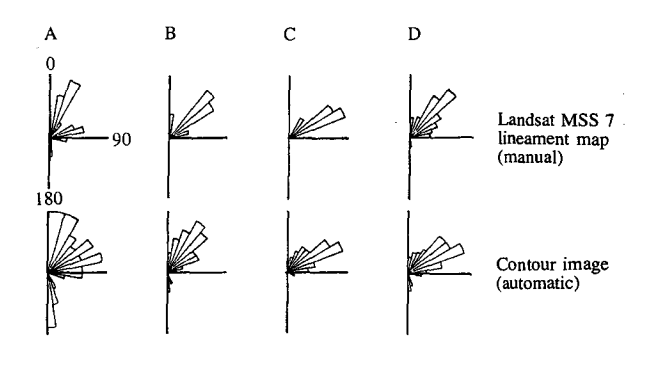
Cevennes region: (a) MSS band 7 of study area. (b) Lineament interpretation map produced from (a). (c) Contour image generated from MSS band 7. (d) Fault map compiled from published sources.

the connection does not appear clearly on the image. Some faults are not seen on the contour image; this is particularly true of faults in the basement, which are identifiable by the interpreter on the basis of texture boundaries alone. It is also true of faults which consist of a succession of small segments, some of which may have been eliminated by the thresholding on the contour image. These differences notwithstanding, a satisfactory correspondence was found between the lineament interpretation map and the automatically generated thresholded contour image. A comparison with the compiled geologic fault map [Figure 3(d) indicates that most of the mapped faults are found on both lineament maps. On the contour image, the faults are represented by short aligned segments, whereas on the lineament interpretation they are more continuous. Faults which are missing on the lineament maps tend to be minor features, with little offset, some thrust faults with complex surface expressions, or faults which are too near to others to be individually resolved.

Four regions, outlined on the MSS 7 image [Fig. 3(a)], have been selected to illustrate the rose diagrams that were produced automatically and manually (Figure 4). The first row shows the rose diagrams computed manually from the lineament interpretation; the second, those produced automatically from the contour image. One can note the good likeness between the rose diagrams corresponding to the same area. Principal directions are the same for rose diagrams drawn from the manual lineament interpretation and the contour image. For example, in area A, the principal directions found on the lineament map are 30, 80, and 170 degrees. On the automatically generated rose diagram, these same directions are prominently seen. The additional peaks at 10 and 60 degrees are due to stream directions, which the interpreter eliminated from the lineament map. In general, however, the rose diagrams produced automatically from the image are in very good agreement with those produced manually.

Multisource data analysis

• Introduction, data utilized, and region studied This section presents a study of the geologic utility of coregistered Landsat and Heat Capacity Mapping Mission (HCMM) data. The data utilized consisted of Landsat MSS data (scene 210–30, acquired June 16, 1980) and visible and thermal data from HCMM (October 31, 1978). The HCMM satellite operated between 1978 and 1980, acquiring images in two spectral bands: the visible and near-infrared (0.5–1.1 μ m), and the thermal infrared (10.5–12.5 μ m). Data were collected during the day and at night, with a ground resolution of 500 m [12]. In addition to the visible and thermal images, a derived image was available, called Apparent Thermal Inertia (ATI). This image is calculated by the formula



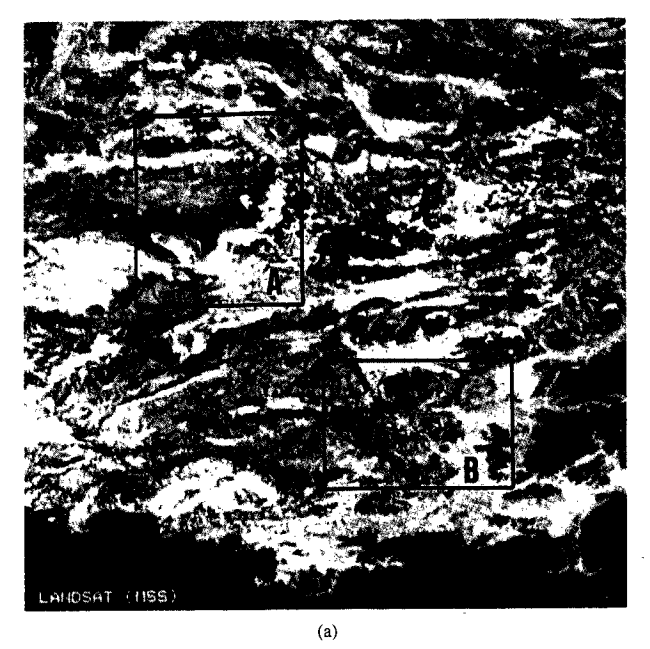
Comparison of rose diagrams of Cevennes region for areas indicated on Fig. 3(a). The diagrams are computed from the lineament interpretation and the contour image.

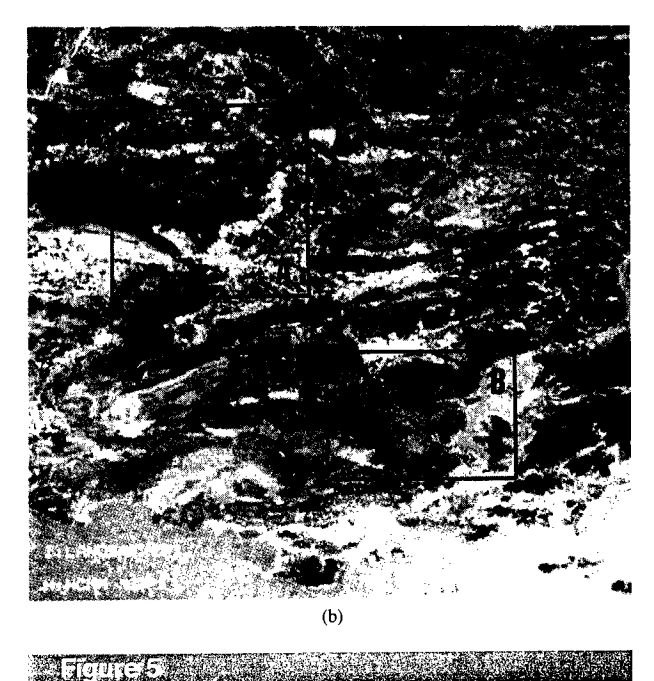
$$ATI = k \frac{1 - albedo}{T_{day} - T_{night}},$$

where $T_{\rm day}$ and $T_{\rm night}$ are the registered day and night temperature images, *albedo* is calculated from the visible and near-infrared image, and k is a scaling factor. Thermal inertia is a calculated physical characteristic of materials which depends on density, specific heat, and conductivity. It has been shown that ATI is a good approximation of thermal inertia and is much easier to calculate [13].

The area studied is the western Provence region of southeastern France (C in Fig. 1). It presents numerous outcrops of light-colored rocks, essentially sandstones, limestones, and dolomites of various ages, which are often difficult to separate even in the field. Vegetation cover varies from 100 percent pine forest cover at higher elevations to more modest cover of 10 to 20 percent at lower elevations. Valleys are typically cultivated or used for cattle grazing.

Landsat MSS data allow separation of materials whose reflectances differ in the visible and near-infrared wavelength regions. It is therefore possible to separate orange to pale red Triassic limestones from white-gray Jurassic limestones and dolomites. But it is very difficult to differentiate Upper Jurassic limestones from dolomites of the same age. Laboratory spectral reflectance measurements of powders show that in the $0.4-1.1-\mu m$ region, dolomite and limestone have practically the same spectral response [14]. A spectroradiometric study done in central France in 1980 [15] presented the spectral responses of typical Triassic sandstone and Cretaceous limestone. Even though their spectral responses were significantly different when broken, fresh surfaces were measured, there was little difference between the responses of their natural surfaces. The visible and nearinfrared reflectances were strongly influenced by the presence





Western Provence study area: (a) Landsat false-color infrared composite, with study areas A and B indicated. (b) Landsat-HCMM composite image; Landsat first principal component as intensity, HCMM night thermal image as hue, and saturation kept constant.

of lichen and the development of surface weathering rinds. On the other hand, the thermal characteristics of limestones and dolomites are distinctly different. Janza [16] reported thermal inertia values for dolomite of 0.075 and for limestone of 0.045, due to large differences of diffusivity and conductivity (thermal inertia is $\sqrt{\kappa\rho c}$, where κ is specific heat, ρ is density, and c is conductivity). For the region studied, therefore, thermal data should serve to improve mapping capabilities for limestone/dolomite terrains.

• Data registration and display techniques

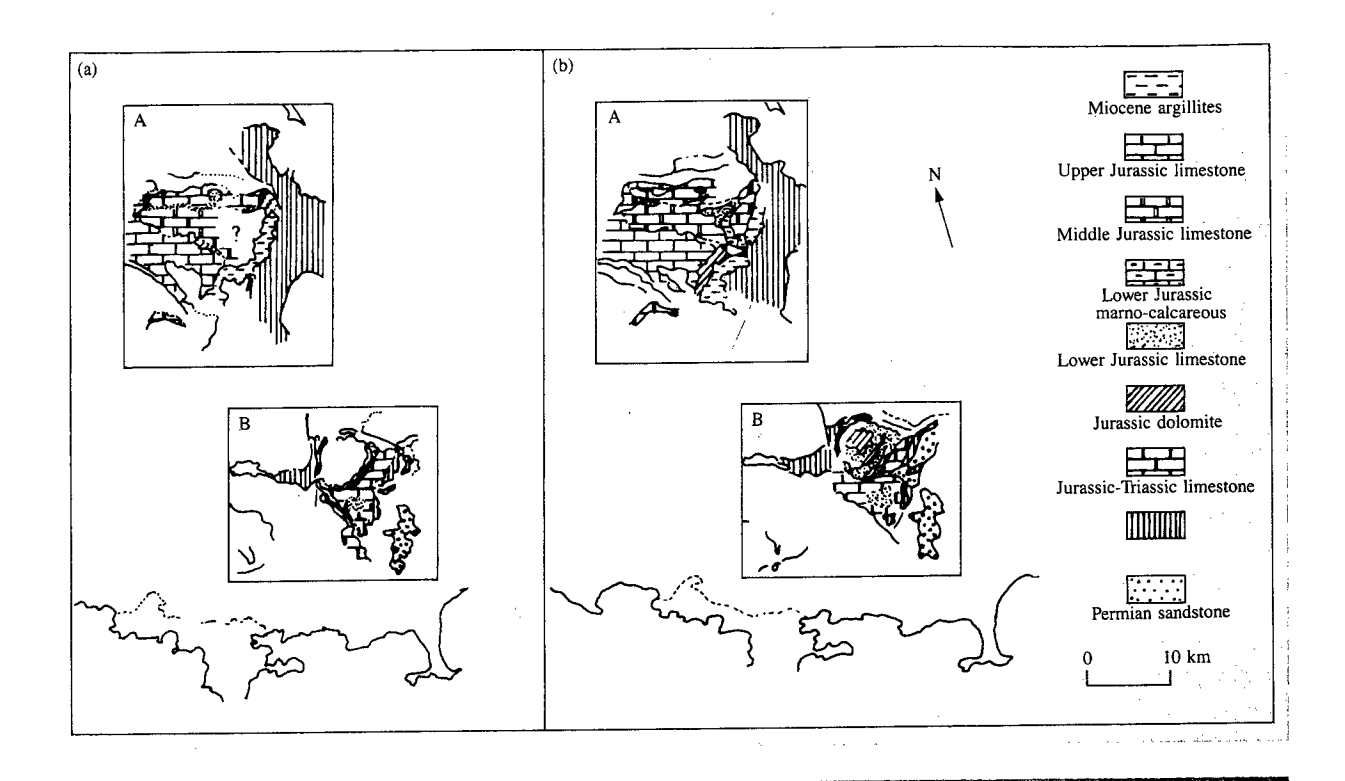
To produce an image combining the data from Landsat and HCMM, it was first necessary to register the two types of data to one another. This was done in three steps: determination of control points, calculation of the deformation model, and resampling. Because of the great disparity in pixel size (80 m versus 500 m), both data sets were resampled to 250 m to facilitate acquisition of ground control points. The two data types were displayed side by side on a display console, and common points were identified on each. The deformation model to transform the HCMM data to the Landsat geometry calculated a fifth-degree polynomial surface which best fit the control points. Finally, the HCMM data were transformed using this model and resampled to 80-m pixels.

There are many techniques available for displaying multivariate image data; the most commonly used is color compositing, using red, green, and blue. The Landsat color composite [Figure 5(a)] was produced in this manner, projecting MSS channels 4, 5, and 7 in blue, green, and red, respectively. The composite Landsat-HCMM image [Figure 5(b)] was produced in a different manner by using the color space intensity, hue, and saturation (IHS). The intensity channel was the first principal component computed from the Landsat channels, the hue information came from the HCMM nighttime thermal image, and saturation was kept constant. The colors are related to nighttime temperatures, and the intensities of the colors are modulated by the first Landsat principal component.

Various visualizations were analyzed by using the ATI image. In all cases composites with this image were less useful than those using the nighttime thermal image. The reason seems to lie in the nature of the ATI image. Because the range and magnitude of the nighttime temperatures are much less than those of daytime temperatures, the difference is not very different from the daytime image minus a constant. The daytime data are very strongly affected by topography and insolation anisotropies, so that they contain very little geologic information, making the ATI images of little use in this region.

• Analysis of images

In certain areas, the Landsat data allow the recognition of formational boundaries, and there are sufficient contours discernible to permit a satisfactory cartography of the geology. In other regions, however, the limits visible on the image are not sufficiently distinct to permit an interpretive



Interpretation maps of Landsat and Landsat-HCMM composite images: (a) Geologic interpretation map of areas A and B based on Landsat image. (b) Geologic interpretation map of areas A and B based on Landsat-HCMM composite image.

in Salah dalah Salah dalah dal

map to be drawn with great confidence. In addition, there are areas where no geologic limits can be detected. Two such regions were selected for analysis by means of the Landsat-HCMM composite to evaluate the additional geologic information obtained by combining reflectance and emittance data. Interpretation maps for the regions based on the Landsat image and the HCMM combined image are shown in **Figure 6**.

The first region (A) is located between St.-Maximin-la-Ste.-Baume and the syncline of Rians; outcrops consist of Jurassic to lower Cretaceous calcareous rocks. The second region (B) is located west of Cuers and is underlain by Triassic to lower Jurassic formations. In area A the formations appear white to light yellow on the Landsat image and are undifferentiable. On the combined image, it is possible to separate the Jurassic formations which are dominantly limestones from those which are marnocalcareous. In addition a zone of dolomitization in the Cretaceous formations appears on the image. In area B two synclines are found, with dolomites stratigraphically above argillites. In the northern syncline, the dolomitized Jurassic rocks are clearly separable from the undolomitized limestones. In the southern syncline, the contact between the Triassic marno-calcareous rocks and the Jurassic dolomites

is visible. None of these contacts are discernible on the Landsat composite.

This example demonstrates a procedure for utilizing two image data sets with greatly different spectral and spatial characteristics. It was found that it is feasible to preserve the data with higher spatial resolution and to resample the data with low spatial resolution to the same pixel size. The IHS display, using Landsat data as intensity and HCMM data as hue, provides an image with the full Landsat resolution. The geologic importance of combining data from a range of spectral intervals is evident from the added discrimination in carbonate terrains. Thermal data are particularly valuable for those rock types whose reflectance signatures are not discriminatory but whose thermal properties are significantly different.

General discussion and remarks

The purpose of image processing applied to remote sensing data for geologic mapping is to provide the geologist with tools (images and registered data) which improve his ability and efficacy in the making of geologic maps. The availability of satellite data in various spectral regions and at different spatial resolutions presents a formidable challenge to extract and display the most useful part of the data, depending on

the problem being addressed. We have presented three new approaches for using remote sensing data. First, we developed processing algorithms to incorporate a textural measure with the spectral information to improve the accuracy of lithologic mapping. By using a series of thematic maps and combining those which were the most accurate, unit by unit, a satisfactory classification map was produced. This technique has wider applications for analyzing different types of data, treating them separately, and then combining the results to produce the final map. In this way, disparate physical measurements of the surface can be used to characterize desired units. Second, we developed a technique to automatically produce lineament maps from image data. This method eliminates the subjective bias inherent in manual image interpretation. The image can be used as is for structural analysis, or the information can be summarized by using the automatic rose diagram program developed. In both cases, the goal is to reduce the amount of time needed to analyze images while trying to reproduce the results arrived at manually. Third, we developed techniques for combining satellite data of greatly different spatial resolution and covering different parts of the electromagnetic spectrum. The two types of data are complementary in that each provides information about surface composition not available in the other. In a dominantly calcareous terrain, thermal data are indispensable for separating the rock types. At the same time, the procedure described allows retention of data of higher spatial resolution when combined with data of much lower resolution.

These are but a few examples of the current developments in image processing technology. The future presents a picture of ever-increasing complexity: New satellite instruments will be launched by several countries, providing a nearly overwhelming quantity of earth observation data. In addition, subsurface data (such as gravimetric and magnetic anomaly maps) must be integrated with the surface data to provide a more complete, three-dimensional picture of the geologic environment. As always, the challenge will be to develop new methods of data processing to extract the maximum of useful information. But we should never lose sight of the fact that this sophisticated technology only provides an additional tool and cannot be used alone for geologic mapping.

Actnowledgments

This paper presents part of the results of a project supported jointly by IBM, the Centre National d'Etudes Spatiales, and the Centre National de la Recherche Scientifique, and conducted at the IBM Science Center, Paris. We wish to acknowledge the participation of Drs. J. Chorowicz and P. Masson of the University of Paris VI and Paris XI. We are also indebted to the personnel of the IBM Scientific Center who were responsible for the development of the HLIPS software package.

References

- "Symposium on Significant Results Obtained from Earth Resources Technology Satellite-1," NASA SP-327, National Aeronautics and Space Administration, Washington, DC, 1973.
- L. Rowan, P. Wetlaufer, A. Goetz, F. Billingsley, and J. Stewart, "Discrimination of Hydrothermally Altered Areas and of Rock Types Using Computer Enhanced ERTS Images, South Central Nevada," *Professional Paper 883*, U.S. Geological Survey, Reston, VA, 1974.
- A. Rosenfeld and A. Kak, Digital Image Processing, Academic Press, Inc., New York, 1976.
- W. Pratt, Digital Image Processing, John Wiley & Sons, Inc., New York, 1978.
- K. Castleman, Digital Image Processing, Prentice-Hall, Inc., Englewood Cliffs, NJ, 1979.
- A. Gillespie, "Digital Techniques of Image Enhancement," Remote Sensing in Geology, B. S. Siegal and A. R. Gillespie, Eds., John Wiley & Sons, Inc., New York, 1980, pp. 139-226.
- P. Franchi, "A System for Color Image Display and Processing," Technical Report G513-3586, IBM Scientific Center, Rome, Italy, 1981.
- 8. L. Asfar, "A Method for Contour Detection, Segmentation, and Classification of Landsat Images," *Proceedings of the International Geoscience and Remote Sensing Symposium*, Washington, DC, June 1981, pp. 298–304.
- B. Siegal and M. Abrams, "Geologic Mapping Using Landsat Data," Photogram. Eng. & Remote Sensing 42, 325-337 (March 1976).
- P. Choukroune and M. Mattauer, "Tectonique des Plaques et Pyrénées: Sur le Fonctionnement de la Faille Transformante Nord-Pyrénéenne; Comparaisons avec des Modeles Actuels," Bull. Soc. Geol. France Series 7 20, No. 5, 689-700 (1978).
- T. Nguyen, S. Simon, L. Asfar, and A. Blusson, "Extraction des Paramétres de Forme pour la Recherche des Structures Linéaires dans les Images-Satellites," *Proceedings, First Image* Colloquium, Biarritz, France, May 1984, pp. 741-746.
- C. Elachi, "Microwave and Infrared Satellite Remote Sensors," *Manual of Remote Sensing*, 2nd ed., R. Colwell, Ed., American Society of Photogrammetry, Falls Church, VA, 1983, Vol. 2, pp. 635-636.
- J. Price, in Heat Capacity Mapping Mission Users' Guide, NASA/Goddard Space Flight Center, Greenbelt, MD, 1978, pp. 8-16.
- G. Hunt and J. Salisbury, "Visible and Near Infrared Spectra of Minerals and Rocks: XI: Sedimentary Rocks," Mod. Geol. 5, 211-217 (1976).
- P. Kuntz, A. Simonin, G. Guyot, and M. Verbrugghe, "Analyse des Signatures Spectrales de Formations Rocheuses du Mont Lozère, France," Proceedings, Congrès Signatures Spectrales d'Objets en Teledétection, Avignon, France, 1981, pp. 147-155.
- F. Janza, "Interaction Mechanisms," Manual of Remote Sensing, R. Reeves, Ed., American Society of Photogrammetry, Falls Church, VA, 1975, Ch. 4, pp. 57-180.

Received July 8, 1984; revised October 1, 1984

Micraest J. Adrams IBM France, 36, Avenue Raymond Poincaré, 75116 Paris, France. Mr. Abrams has just completed a one-year position as visiting scientist, working on the joint IBM/CNES/CNRS geology remote sensing project. From 1973 to 1983, he was a staff scientist at the NASA/Jet Propulsion Laboratory, Pasadena, California, and principal investigator for several NASA-funded research studies on the applications of remote sensing for geology. He received a B.S. with honors in biology in 1970 and an M.S. in geology in 1973, both from the California Institute of Technology, Pasadena. Mr. Abrams is a recipient of NASA's Group Achievement Award. He is a member of the National Academy of Science Space Science Advisory board and the Society of Economic Geologists.

Annick Blusson IBM France, 36, Avenue Raymond Poincaré, 75116 Paris, France. Ms. Blusson is presently completing her Doctorat de 3^{eme} Cycle in structural geology and remote sensing at the University of Paris (XI) while participating in the joint IBM/CNES/CNRS remote sensing geology project.

Veronique Carrera IBM France, 36, Avenue Raymond Poincaré, 75116 Paris, France. Ms. Carrere received her Doctorat de 3^{eme} Cycle in structural geology and remote sensing from the University of Paris (VI). She is presently completing her thesis for the Doctorat d'Etat (Ph.D) while participating in the joint IBM/CNES/CNRS remote sensing geology project.

Phu Thien Nguyen IBM France, 36, Avenue Raymond Poincaré, 75116 Paris, France. Dr. Nguyen received his B.E. and M.E. degrees in 1967 and 1969 from the University of Canterbury, New Zealand, and his Ph.D. in 1977 in agricultural engineering from the University of Newcastle-upon-Tyne, United Kingdom. Before joining the Scientific Center in 1978, he was the head of the Agricultural Engineering Department at the University of Can Tho, Viet Nam. He is currently technical manager of the joint IBM/CNES/CNRS geology remote sensing project. His research interests are in digital image processing, pattern recognition, and image processing applied to geology, agriculture, and urban planning.

Yves Rabu IBM France, 36, Avenue Raymond Poincaré, 75116 Paris, France. Mr. Rabu received his Maitrise in geology from the University of Nantes in 1981 and his D.E.A. in remote sensing from the Center for Space Studies (CESR, University Paul Sabatier, Toulouse) in 1982. He is currently completing a thesis for the Doctorat de 3 cme Cycle at the University of Paris (IV) on the development of image processing techniques for geologic mapping. He is also participating in the joint IBM/CNES/CNRS geology remote sensing project.